International Journal of Applied and Structural Mechanics
ISSN: 2799-127X
Vol: 04, No. 05, August-September 2024
http://journal.hmjournals.com/index.php/IJASM
DOI: https://doi.org/10.55529/ijasm.45.11.24

An Examination of the Electronic, Optical, and Thermodynamic Properties of B-Gan

Aya Farman Noori[1*], Abdulhadi Mirdan Ghaleb[2], Ali Ismail Salih[3]

[1]Master student, Department of Physics, College of Sciences, University of Kirkuk, Kirkuk, Iraq.*
[2,3]Professor, Department of Physics, College of Sciences, University of Kirkuk, Kirkuk, Iraq.

Email: [2]abdlhadik@uokirkuk.edu.iq, [3]aliismailsalih@uokirkuk.edu.iq
Corresponding Email: [1]scpm23012@uokirkuk.edu.iq*

Received: 29 May 2024 **Accepted:** 14 August 2024 **Published:** 30 September 2024

Abstract: ***The current work involves the systematic examination of the features of Gallium Nitride (GaN) including the electronic, optical, structural, and thermodynamic features, depending on first principles calculation. This is according to approximations, (LDA), (GGA), and (m-GGA). The bandgap energies of Gallium nitride are (1.85 eV, 1.93 eV, and 2.179 eV), respectively. Furthermore, our study also reveals that GaN has a direct bandgap and is highly stable. Finally, our results indicate that the m-GGA method accurately predicts the bandgap energy of GaN. The m-GGA method outperforms both LDA and GGA methods in accuracy to predict the bandgap energy of GaN, as evidenced by its closest approximation to the experimental value. To determine the orbital nature of the Gallium and Nitrogen atoms, the state density and state partial density of Gallium nitride were simulated. The absorption coefficient of Gallium nitride is computed and analyzed in depth for the optical transitions. The absorption coefficient of Gallium nitride is affected by various factors, including the material's band structure, temperature, doping level, and the energy of the incident photons. In addition to that, the thermodynamic properties that can be calculated like enthalpy, entropy, heat capacity, free energy, and Debye temperature enable us to understand the thermal behavior of the compound better. The heat capacity of α-GaN is detected to be (39.9, 25.5, and 32.4) Jmole-1K-1, and a Debye temperature of 807 K, 1134 K, and 866 K for LDA, GGA, and m-GGA, respectively. This research will offer a detailed interpretation of β-GaN, covering all its basic properties and possible applications in electronic devices and optoelectronic devices. The results of this study are very important and the new technologies that will be developed based on the Cubic phase - GaN research will be very beneficial.***

Keywords: ***B-Gan, Structural, Electronic, Optical Properties, and Thermodynamic Properties.***

International Journal of Applied and Structural Mechanics
ISSN: 2799-127X
Vol: 04, No. 05, August-September 2024
http://journal.hmjournals.com/index.php/IJASM
DOI: https://doi.org/10.55529/ijasm.45.11.24

1. INTRODUCTION

Zinc-blende GaN semiconductor materials are not only applied generally in light emitting diode (LED), laser emitting diode, photodetectors, and photoelectric modulators but also used with the fundamental materials for cementing hetero-structures, superlattice structures, as well as quantum-well structures. The research of the energy structure for the crystal or the effective carrier mass may involve theoretical computation or experimental methods that can offer a theoretical foundation and practical reference for the new semiconductor material. The relative measure of the efficiency of the photoelectric conversion, the mobility of the carriers proportional to their concentration, excitation energy levels, and acceptor impurities are correlated to the degenerate state at the end of the valence band [1] [2]. The effective mass and basic energy gap of zinc-blende GaN is calculated by several investigators in recent years as follows, [3] utilized a full-potential linear amplified plane-wave model to test electronic, effective mass properties and structure of zinc-blende group-III nitride and compounds of silicon semiconductor as well as [4] used the same model to study crystal symmetry and optical gain in III–V nitride lasers. [5] By empirical pseudopotential method, and [6] with the k.p method. Although there are many experimental studies and theoretical research on the electronic structure of zinc-blende GaN [7] [8] [9] [10] [11] [12], the work has been limited to studying only the dielectric function and absorption coefficient. According to previous studies, GaN may have been structured as zinc-blende as the element determining GaN semiconductor, many previous studies have extensively investigated the electronic GaN crystals features.[13] S orbital of Ga near the Fermi and P orbital of N levels are responsible for the electrical transport and GaN carriers according to research on the electronic structure and photoelectrical characteristics of zinc-blende. [5] Reached the zinc-blende GaN´s electrical characteristics and their findings demonstrated that the material is a direct-gap semiconductor. Among the previous studies that have examined (LDA and GGA) approximations for crystal systems, both cubical and hexagonal [14] [15] [16]. This work investigates the structural, optical, electronic, and thermodynamic β-GaN features through the first principle of DFT calculations.

2. RELATED WORKS

[15] Examines the structural, elastic, electronic, and optical properties of ZnSe using plane-wave pseudopotential formalism and density functional theory, with LDA and GGA as exchange-correlation potentials (DFT). The optimal structure of the binary semiconductor ZnSe crystallized in the complex sphalerite phase was determined by analyzing energy as a function of basic unit volume. The calculated equilibrium lattice constants, bulk moduli, and volumes are reasonably consistent with the experimental results. The band structure, density of states, and Mulliken population were calculated to investigate the electronic and chemical bonding properties, respectively. We discovered that for ZnSe, the band gap of LDA is 1.33 eV and that of GGA is 1.34 eV. Additionally, optical properties (absorption coefficients) were calculated , [17] β-GaN's optical, elastic constant, and electronic characteristics have all been investigated using the ab initio pseudopotential (PP) method within the generalized gradient approximation (GGA). They obtain squeezed energy bands around the fermi level, higher DOS, and an underestimated band gap. To compute electronic band structures, the d-band effect is

International Journal of Applied and Structural Mechanics
ISSN: 2799-127X
Vol: 04, No. 05, August-September 2024
http://journal.hmjournals.com/index.php/IJASM
DOI: https://doi.org/10.55529/ijasm.45.11.24

briefly discussed. Acoustic wave speeds in the (100), (110), and (111) planes are computed with the aid of elastic constants. Its pressure coefficient, refractive index, and dielectric constant are all clearly shown. For each of these characteristics, the hydrostatic pressure effect is explained. The current experimental and first-principle computations are used to assess the study's findings. [18]They studied the theory of the piezoelectric, elastic, electronic, and structural characteristics of zinc-blende AlN and GaN about pressure. The study focuses on the density functional theory first-principles calculations of all electron full potential augmented plane waves plus local orbitals. Both the generalized gradient approximation (GGA) and the local density approximation (LDA) are used to obtain and compare the results of bulk properties, such as lattice constants, bulk modulus, derivatives, and band structures for the exchange-correlation functional. We discover that there is no discernible improvement over LDA using GGA. Under hydrostatic pressure, the electronic energy levels and ionicity factors are examined. They expand their research to include a study of the impact of stress on transverse effective charges and piezoelectric constants. The sign of the piezoelectric constants in III–V nitrides is similar to that of II-VI compounds. With pressure, the transverse effective charges and piezoelectric constants change nonlinearly. [19]DFT-based first principle calculations are used to study the electronic and optical properties of zinc blende and wurtzite structure GaN. Zinc blend and wurtzite GaN differences are compared, and the (partial) density of states (DOS) is computed. The wurtzite structure has a wider band gap due to its significantly lower DOS around the Fermi level than the zinc bend structure, according to the results. Under both normal and high external pressure, the complex refractive indices and the absorption coefficients are computed. According to the results, wurtzite GaN is a better material for blue light emission.

3. METHODOLOGY

Computational Method

This paper presents the results of calculations by the density functional theory (DFT) plane-wave pseudopotential, incorporated into the Castep Code [20] using norm-conserving pseudopotentials [21], and the wave functions extended as a plane wave. The Ceperley Alder Predew Zunger$(CAPZ)$technique was utilized by LDA to characterize the exchange-correlation potential to get a rough approximation of E_{XC} [22], and generalized gradient approximation GGA [23], with the $PBESOL$ scheme, and Meta generalized gradient approximation $m-GGA$ [24]. Calculations using pseudo-atoms are carried out on (Ga:$3d^{10}4s^2$, (N: $4\,s^2 4p^4$. The convergence of all energies in a self-consistence manner is$(1.0\,x\,10^{-5})\,eV\,/\,atom$. To verify calculation convergence, we closely analyze the cut energy and whole energy dependence on the k-point set grid following the Monkhorst-Pack grid. To illustrate the computational effort, a basic set of plane waves with a cutoff energy of 1115.70eV forLDA, 590eV for GGA and 880 eV for $m-GGA$ (RSCAN) is applied and the (6 x 6 x 6) (LDA) (1x1x1) $(GGA)$and (1x1x1) $(m-GGA)$k-point Monkhorst Pack mesh is in the Brillouin zone. Utilized for K-point sampling (BZ). The extreme force between atoms convergence criterion $0.03\,eV\,/$ Å the displacement 0.001Å and the strain$0.05GPa$. Mullikan charges were examined for all equilibrium structures by plane wave state projections onto linearly combined atomic orbital sets frequently employed for population analysis and charge

International Journal of Applied and Structural Mechanics
ISSN: 2799-127X
Vol: 04, No. 05, August-September 2024
http://journal.hmjournals.com/index.php/IJASM
DOI: https://doi.org/10.55529/ijasm.45.11.24

transfer [23][24]. The optimized structure performed optical features, electronic band structure, and the states DOS spectrum density.

4. RESULTS AND DISCUSSIONS

Structure Properties

β-GaN is of the the $F-43M$ (216)space family; $a = b = c = 0.45\ nm$ [27]and $\alpha = \beta = \gamma = 90^{\circ}\wedge\circ$ can be used to described the lattice constant. N atoms are located in the 1/4 position of the body diagonal. Ga atoms are in eight corners and six centers of faces. Four Ga and four N atoms can be found in each cell. The minimization of the total energy has optimized the lattice constants and atomic positions as a normal stress. In Figure 1 the optimized structure is displayed. Table 1 displays the determined values of Zinc-blende GaN´s structural features in addition to the experimental values [28], [29] and additional results [27], [30]. Table 1 shows that the theoretical results we currently agree with the experimental and other theoretical results. The current work's computed lattice constant is 4.498Å(LDA) 4.508 Å (GGA),and 4.496Å $(m-GGA)$as a result of the various calculations of techniques, exhibits a 0.74% deviation from the experimental values and is somewhat bigger than other the data from the theory. This demonstrates the accuracy of our current first-principles DFT-based computations.

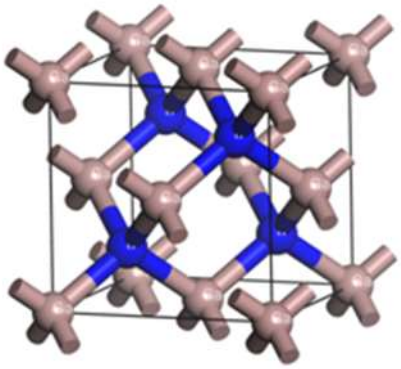

Fig. 1 the Traditional Cubic Cell B-Gan Crystal Structure.

Table. 1 The Lattice Parameters For B-Gan In The Cubic Phase Were Compared Between The Calculated Value And The Experimental One. The Calculated Values Were Determined Using Different Approximations Such As LDA, GGA, And M-GGA.

Phase	Approach	$\mathbf{a}_{\circ} = \mathbf{b}_{\circ} = \mathbf{c}$ (Å)	V(Å)	Reference
β-GaN	LDA	4.498	91.027	present work
	GGA	4.508	91.666	
	m-GGA	4.496	90.851	
	LDA, GGA	4.558	94.694	[31]
	molecular-dynamics simulations	4.528	92.83	[32]
	Experiment	4.50	91.125	[33]
	Experiment	4.510	91.733	[30]

International Journal of Applied and Structural Mechanics
ISSN: 2799-127X
Vol: 04, No. 05, August-September 2024
http://journal.hmjournals.com/index.php/IJASM
DOI: https://doi.org/10.55529/ijasm.45.11.24

Electronic Structure

The Castep software is used to generate k-points along high symmetry by following the k-path for determining the band structures. Figure 2 (a, b, c) displays the energy band structure of bulk GaN using both approximations (LDA, GGA, and m-GGA) within the functional theory of densities. One method of identifying the differences in the electrical characteristics of metals, semiconductors, and insulators is to look at the energy gaps between (un)occupied energy levels. The conduction band is over the Fermi levels and the valence beneath it. The band gap has been computed as the variation energy between the maximum band of valence and the minimum of conduction band. We determined the energy of the band gaps from the three-dimensional GaN band structure, which is (1.85eV for LDA, 1.93eV for GGA, and 2.17eV for m-GGA), lower than with other theoretical [34] and with the experimental value $E_g = 3.3eV$ [35], as a result of the ground state theory being employed in the DFT computation, whereas the excited state is represented by the energy gap. Thus, the result decreases, particularly in the band gap between the insulators and semiconductors. It differs by $30-50\%$from the experimental value.

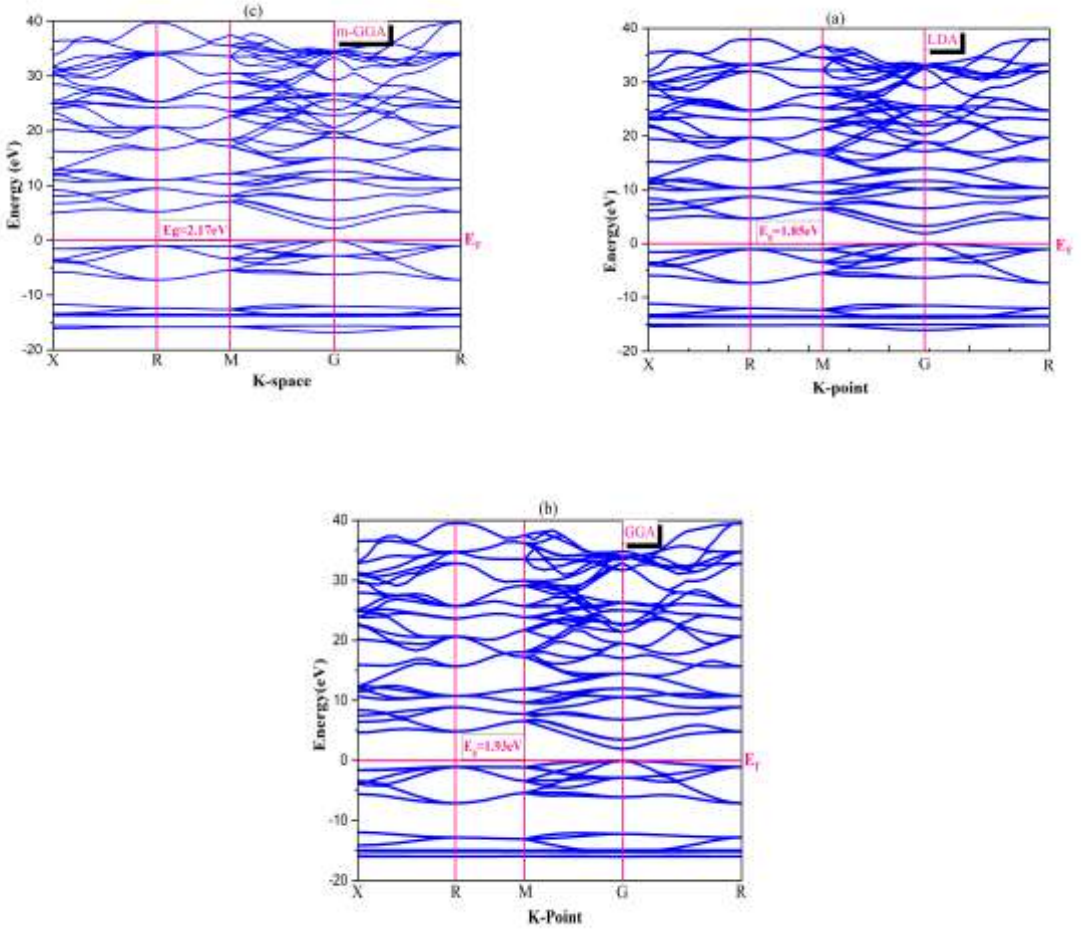

Fig. 2 The Gan Band Structures In The Beta Phase Win (A) LDA, (B) GGA, And (C) M-GGA Methods.

International Journal of Applied and Structural Mechanics
ISSN: 2799-127X
Vol: 04, No. 05, August-September 2024
http://journal.hmjournals.com/index.php/IJASM
DOI: https://doi.org/10.55529/ijasm.45.11.24

Table 2 The Beta Phase Energy Band Gap (Eg) Of B-Gan Has Been Measured By Several Techniques, Including M-GGA, GGA, And LDA.

Phase	Approach	E_g (eV)	Reference
	LDA	1.85	Present work
	GGA	1.93	
β -GaN	m-GGA	2.179	
	Other theoretical work	3.1	[31]
	Experiment	3.3	[33]

Density of States

The two types of state densities are total (TDOS) and partial (PDOS) for β-GaN are displayed in Figure 3 (a, b, and c) (TDOS) and Figure 4 (a, b, and c) (PDOS) calculated using three approximations (LDA, GGA, and m-GGA). The result show that the valence bands for GaN are of two sections, specifically the upper the valence bands between $(-7.5eV)$and $(0eV)$and between the bands of lower valences $(-16.2eV)$and $(-11.1eV)$. When the valance bands are lower, PDOS of GaN is mostly occupied by the (N–2s) and $(Ga-3d)$states, during hybridization, the minor is contributed by the $(N-2p)$ and $(Ga-4s)$states. The $(Ga-3d)$states occupy in the range of $(-16.2 \sim -13.2)eV$ while $N-s$ states occupy in the range of $(-13.2 \sim -9.1)eV$ According to Figure 3 , GaN exhibits a sharp peak at $-13.0eV$ suggesting that a greater number of $Ga-3d$ state, in the hybridization process electrons are involved for GaN making sturdy localized states. At the upper valence bands, PDOS for GaN is fundamentally filled by the $(N-p)$and $(Ga-3d)$ states, where the contribution of $N-p$ it is greater than that of $(Ga-4p)$demonstrating significant delocalization. As we approach the Fermi level, the $(N-p)$and $(Ga-4p)$states occupy the majority of TDOS for GaN. In addition, Figure 3 (a, b, and c) shows the GaN conduction bands are in the range of $(4.1\sim 12.1)$ eV and $(0 \sim 7.2)$ eV largely consisting of the $(Ga-4s)$and $(Ga-4p)$states. However, at the band lower sections of the, the anti-bonding states of $(Ga-4s)$ are evident. Then, electrons associated with $(Ga-4s)$and $(Ga-4p)$shift toward the mass of the localized N atoms because of the hybridization from $(N-sp)$ to $(Ga-4s)$. Figure 3 (a, b, and c) shows that the TDOS for GaN is markedly different from semiconductor GaP, GaAs, and GaSb. This may be because the electro-negativity of N is greater than that of P, As, and Sb. Our interpretations are consistent with previous sources to references[13][36].

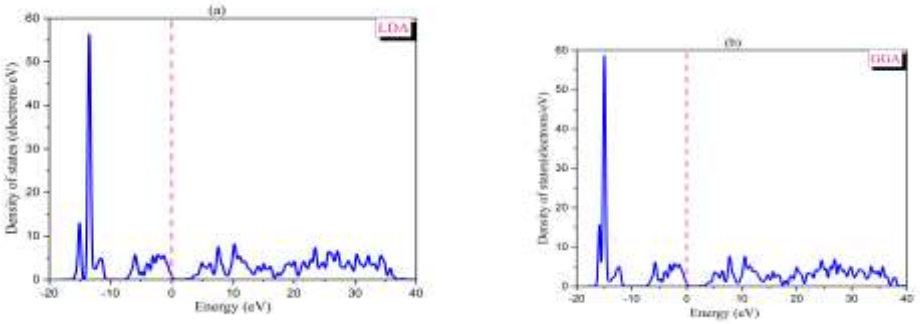

International Journal of Applied and Structural Mechanics
ISSN: 2799-127X
Vol: 04, No. 05, August-September 2024
http://journal.hmjournals.com/index.php/IJASM
DOI: https://doi.org/10.55529/ijasm.45.11.24

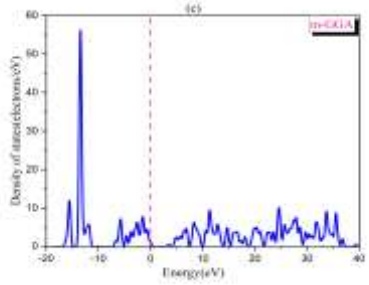

Fig. 3 The Total DOS of B-Gan Using Functional (A) LDA, (B) GGA, and (C) M-GGA.

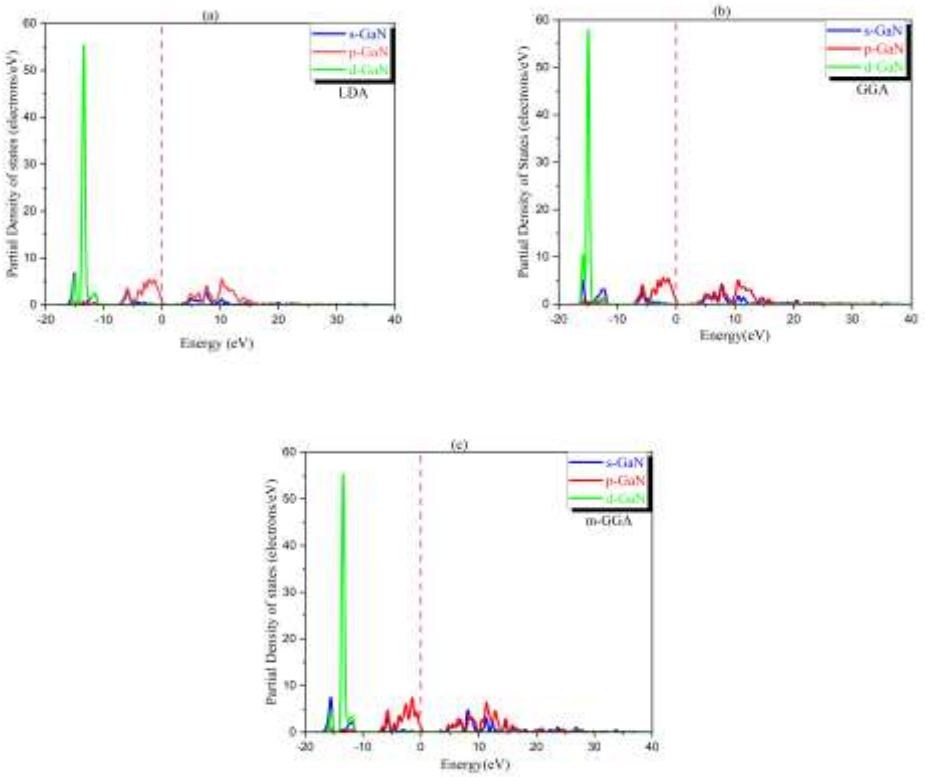

Fig. 4 The Part DOS Of B-Gan Using Functional (A) LDA, (B) GGA, And (C) M-GGA.

Optical Properties

The light absorption coefficient indicates how much the intensity of light decreases as it travels through a medium over a certain distance. The absorption spectrum of GaN is determined using Equation (1):

$$\alpha = \frac{2\omega k}{c} = \frac{4\pi k}{\lambda_0} \qquad (1)$$

Figure 5 illustrates that the absorption is zero when the energies are equal to 1.85eV, 1.93eV and 2.179eV (LDA, GGA, and m-GGA) all greater than 45 eV (m-GGA), 47 eV (LDA) and

International Journal of Applied and Structural Mechanics
ISSN: 2799-127X
Vol: 04, No. 05, August-September 2024
http://journal.hmjournals.com/index.php/IJASM
DOI: https://doi.org/10.55529/ijasm.45.11.24

48 eV (GGA). When a photon energy exceeds1.85 eV, 1.93eV and1.93eV, the absorption coefficient increased, identical to the modified bandgap. It peaks at 396545.5cm-1 (LDA), 398855.5cm-1 (GGA), 389950.5 cm-1 (m-GGA) when energy is at 12.22 eV,10.7426 eV,11.2eV, respectively, and decreased to zero as photon energy exceeds 12.22 eV This indicates that GaN exhibits an absorption coefficient around 〖10〗^5 〖cm〗^(-1)and has a very sharp cut-off response in the ultraviolet range. Our results were compared with experimental results [37], and with other theoretical results [13], we observed good agreement between the calculations.

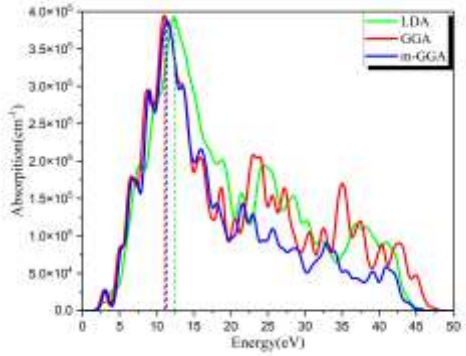

Fig. 5 Absorption Coefficients Are Computed By Lda, Gga, And M-Gga.

Thermodynamic Properties

Various thermodynamic features: Debye temperature, enthalpies, free energies, entropies, and heat capacities, were analyzed to explore alterations in thermal characteristics at zero pressure. The Debye temperature [38] signifies the peak vibration mode of the crystal when phonon vibrates. At zero pressure by the calculated phonon state density employing quasi-harmonic estimates. The following equations have been used to calculate the phonon addition to the Helmholtz free energy F, the entropy E, enthalpy S, and the constant-volume precise heat Cv [39]:

$$\mathrm{F} = 3nNK_BT \int_0^{\omega_{max}} ln\left\{2sinh\frac{\hbar\omega}{2K_BT}\right\} g(\omega)d\omega \quad (1)$$

$$\mathrm{E} = 3nN\frac{\hbar}{2} \int_0^{\omega_{max}} \omega coth\left(\frac{\hbar\omega}{2K_BT}\right) g(\omega)d\omega \quad (2)$$

$$\mathrm{S} = 3nNK_B \left[\int_0^{\omega_{max}} \frac{\hbar\omega}{2K_BT}\ \omega coth\left(\frac{\hbar\omega}{2K_BT}\right) - ln\left\{2sinh\frac{\hbar\omega}{2K_BT}\right\}\right] g(\omega)d\omega \quad (3)$$

$$\mathrm{C_v} = 3nNK_B \int_0^{\omega_{max}} (\frac{\hbar\omega}{2K_BT})^2\ csch^2\left(\frac{\hbar\omega}{2K_BT}\right) g(\omega)d\omega \quad (4)$$

International Journal of Applied and Structural Mechanics
ISSN: 2799-127X
Vol: 04, No. 05, August-September 2024
http://journal.hmjournals.com/index.php/IJASM
DOI: https://doi.org/10.55529/ijasm.45.11.24

$$\theta_D = \frac{h}{K_B}\left[\frac{3m}{4\pi}\left(\frac{N_A\rho}{M}\right)\right]^{1/3} v_m \quad (5)$$

In the expression, the Planck's constant, denoted by h, and the Boltzmann constant, denoted by kB, are used. The unit cell volume is V, while n signifies the number of atoms within a unit cell, and vm indicates the average sound velocity which can be calculated by the equation provided [40].

$$v_m = \left[\frac{1}{3}\left(\frac{2}{v_t^3} + \frac{1}{v_l^3}\right)\right]^{-\frac{1}{3}} \quad (6)$$

The transverse and longitudinal sound velocities are vt and vl respectively estimated by utilizing modulus of the bulk values, B, and of the shear, G. This estimation can be achieved through the application of the following expression [40].

$$v_l = \left(\frac{B + \frac{3}{4}G}{\rho}\right) \text{ and } v_t = \left[\frac{G}{\rho}\right]^{\frac{1}{3}} \quad (7)$$

Figure 5 illustrates the free energy, the thermodynamic potentials' enthalpy profiles, the temperature times and the entropy, TS = U − F, with respect to temperature (in K) for β-GaN, utilizing functional LDA, GGA, and m-GGA. It can be observed that the enthalpy (solid blue line) shows a nearly linear trend in relation to temperature, while the free energy (solid red line) experiences a slight decrease until 380 K, followed by a linear pattern with increasing temperature. As expected, the term TS (solid green line) demonstrates significant growth as temperature increases.

Thermodynamic potentials, such as enthalpy and free energy, play pivotal roles in understanding the behavior of physical systems. By considering the interplay of these potentials with entropy, scientists can make predictions about the spontaneity and feasibility of processes. As we continue to explore the intricacies of thermodynamics, these concepts will remain fundamental in our quest for a deeper understanding of nature's laws.

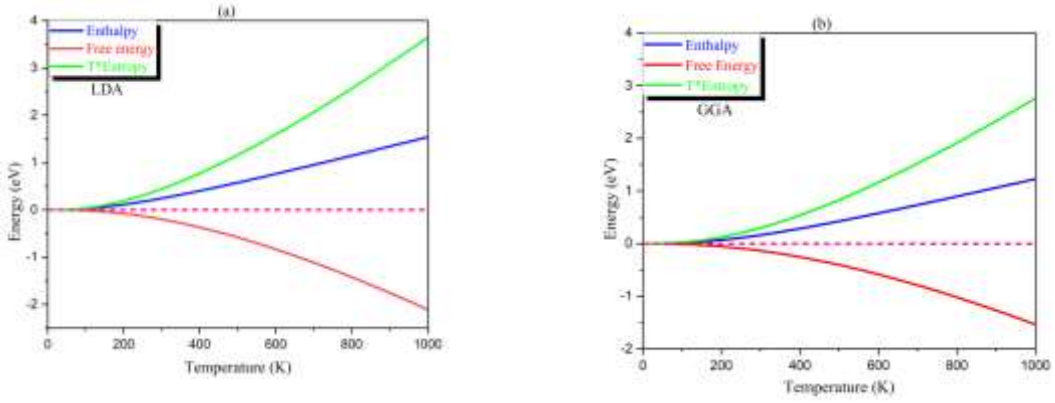

International Journal of Applied and Structural Mechanics
ISSN: 2799-127X
Vol: 04, No. 05, August-September 2024
http://journal.hmjournals.com/index.php/IJASM
DOI: https://doi.org/10.55529/ijasm.45.11.24

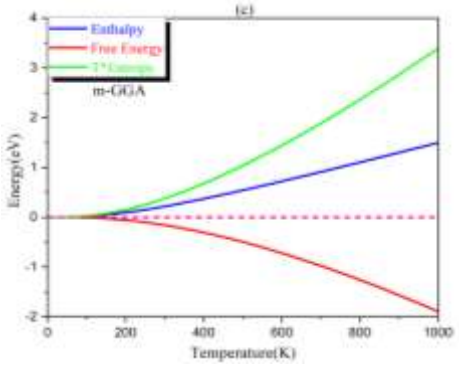

Fig. 6 Enthalpy, Free Energy, And Entropy Of The B-Gan Phase Using (A)LDA, (B)GGA, And (C)M-GGA, Respectively All Calculations In The Range 0–1000K.

The heat capacity obtained through the LDA, GGA, and m-GGA techniques is illustrated in Figure 6 There is a clear power-law temperature correlation observable for the heat capacity at lower temperatures. The calculated power-law exponent of the two GaN crystals is 3, similar to the Debye heat capacity theory. Apart from this, the heat capacities of LDA at 300 K were calculated to be 34.1 J mole-1K-1, GGA gave 25.38 J mole-1K-1 and m-GGA obtained a value of 32.2 J mole-1K-1. The experimental heat capacity of β-GaN being 34.9 J mole-1K-1 at 300 K, the fitted parameters are close to those of the 300 K range [36]. This means that the GaN crystal has an effective heat capacity of 23.6 J mole–1K–1, called the Dulong–Petit limit. This value is characteristic of materials at elevated temperatures. It obviously comes to our view that the thermal capacity and the heat capacities of GaN crystals do not show any variation from 0 to 1000 K, signifying that the structure of crystal in GaN does not influence it. The heat capacity of β-GaN is affected by several parameters not the least of which are those due to lattice vibrations, crystal distortion, and the existence of impurities and defects. In addition to that phonon mean free path that gives the ability of lattice vibrations to travel an expected distance before the occurrence of scattering also influences the heat capacity of β-GaN.

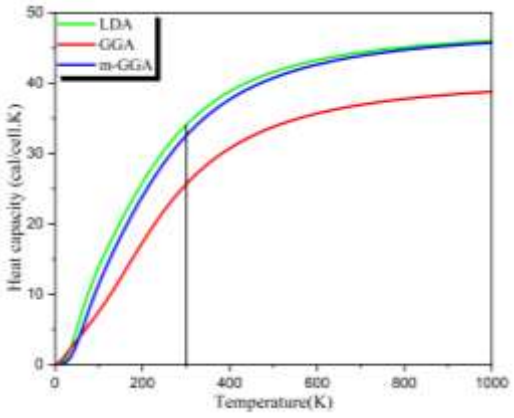

Fig. 7 Depicts The Heat Capacity Determined By LDA, GGA, And M-GGA Methods.

International Journal of Applied and Structural Mechanics
ISSN: 2799-127X
Vol: 04, No. 05, August-September 2024
http://journal.hmjournals.com/index.php/IJASM
DOI: https://doi.org/10.55529/ijasm.45.11.24

The relationship between the Debye temperature and temperature is illustrated in Figure 8. The Debye temperature serves as an indicator of the bonding strength among atoms and consequently correlates with the material's hardness. Typically, a greater Debye temperature signifies a higher level of hardness [41]. When the Debye temperature dependence is tested based on temperature under zero pressure conditions, it becomes evident that the GaN crystal undergoes softening. However, the application of pressure can counteract this softening effect. The Debye temperature ΘD at room temperature is determined to be 395 K. It is observed in Figure 5 that pressure has a more pronounced impact on ΘD compared to temperature. Additionally, the Debye temperatures of GaN exhibit variability, with previous research indicating values ranging from 600 K to 800 K for β-GaN [42]. In the current investigation, the calculated Debye temperatures for β-GaN are 735 K, 1100 K, and 760 K for LDA, GGA, and m-GGA, respectively, at 300 K.

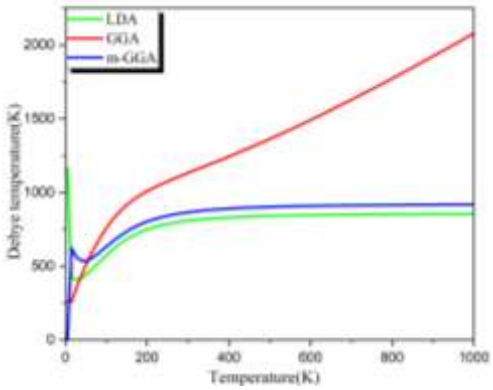

Fig. 8 Debye Temperature of the B-Gan, Using Functional LDA, GGA, and M-GGA.

5. CONCLUSIONS

We offer a thorough analysis of β-GaN structural, electronic, optical, and thermodynamic properties in this work. The LDA, GGA, and m-GGA approximations were used in the computation of the pseudo-potential plane waves (PP-PW), which is a method according to the DFT and used in the Castep code. The calculation of the electronic band of this compound reveals a direct band gap. In contrast, the total and partial density of states (DOS, PDOS) and the optical constants, α (ω) have also been computed. The quasi-harmonic approximation was utilized to compute the temperature dependence of a few parameters including Debye temperatures, enthalpies, free energies, entropies, and heat capacities for β-GaN. Two different methods, such as LDA and GGA approaches were used in this research to obtain the energy band gap in which the electronic band gap and the gap between the valence band and the conduction one were 1.85eV and 1.93eV respectively. Also, the result of the m-GGA showed a band gap (2.179 eV). Both the LDA and GGA methods have underestimated the energy band gaps, however, the m-GGA method has resolved this conflict and provides results that nearly agree with the experimental works. In addition, the m-GGA method has been demonstrated to be efficient because of its capability to accurately describe the electronic states. In the last, the conclusion is made that the m-GGA is an exceptional tool for computing the essential electronic structure of β-GaN which means that the material is appropriate for optoelectronic

International Journal of Applied and Structural Mechanics
ISSN: 2799-127X
Vol: 04, No. 05, August-September 2024
http://journal.hmjournals.com/index.php/IJASM
DOI: https://doi.org/10.55529/ijasm.45.11.24

applications. Not only the simulation is acknowledged to have a close relationship to the experimental and theoretical results, but it is also considered to be a very good prediction for the investigation that may be conducted in the immediate future.

6. REFERENCES

1. Ji. Pankove, J. E. Berkeyheiser, H. P. Maruska, and J. Wittke, "Luminescent properties of GaN," Solid State Commun., vol. 8, no. 13, pp. 1051–1053, 1970.
2. J. I. Pankove, "Luminescence in GaN," J. Lumin., vol. 7, pp. 114–126, 1973.
3. L. E. Ramos, L. K. Teles, L. M. R. Scolfaro, J. L. P. Castineira, A. L. Rosa, and J. R. Leite, "Structural, electronic, and effective-mass properties of silicon and zinc-blende group-III nitride semiconductor compounds," Phys. Rev. B, vol. 63, no. 16, p. 165210, 2001.
4. M. Suzuki and T. Uenoyama, "Strain effect on electronic and optical properties of GaN/AlGaN quantum-well lasers," J. Appl. Phys., vol. 80, no. 12, pp. 6868–6874, 1996.
5. W. J. Fan, M. F. Li, T. C. Chong, and J. B. Xia, "Electronic properties of zinc-blende GaN, AlN, and their alloys Ga1− x Al x N," J. Appl. Phys., vol. 79, no. 1, pp. 188–194, 1996.
6. D. Ahn, "Optical gain of InGaP and cubic GaN quantum-well lasers with very strong spin–orbit coupling," J. Appl. Phys., vol. 79, no. 10, pp. 7731–7737, 1996.
7. R. Miotto, G. P. Srivastava, and A. C. Ferraz, "First-principles pseudopotential study of GaN and BN (110) surfaces," Surf. Sci., vol. 426, no. 1, pp. 75–82, 1999.
8. H. Wang, H. Xu, N. Zhang, and P. Zhang, "The dielectric and dynamical properties of zinc-blende BN, AlN and GaN from first-principle calculation," Sci. China Ser. G Physics, Mech. Astron., vol. 51, no. 8, pp. 1037–1045, 2008.
9. S. Li and C. Ouyang, "First principles study of wurtzite and zinc blende GaN: A comparison of the electronic and optical properties," Phys. Lett. Sect. a Gen. At. Solid State Phys., vol. 336, no. 2–3, pp. 145–151, 2005, doi: 10.1016/j.physleta.2005.01.009.
10. J.-Y. Guo, G. Zheng, K.-H. He, and J.-Z. Chen, "First-principles study on electronic structure and optical properties of Al and Mg doped GaN," 2008.
11. R. Y. Korotkov, J. M. Gregie, and B. W. Wessels, "Electrical properties of p-type GaN: Mg codoped with oxygen," Appl. Phys. Lett., vol. 78, no. 2, pp. 222–224, 2001.
12. D. Cai, X. Feng, Z. Zhu, and J. Kang, "Electronic Structures of Zinc-Blende GaN (001) Surface," CHINESE J. Semicond. Ed., vol. 22, no. 11, pp. 1400–1404, 2001.
13. Y. Du, B. Chang, X. Fu, X. Wang, and M. Wang, "Electronic structure and optical properties of zinc-blende GaN," Optik (Stuttg)., vol. 123, no. 24, pp. 2208–2212, 2012.
14. A. Shihatha, A. Ghelab, and R. Munfi, Theoretical study of electronic structure and optical properties for ZnO thin film, vol. 2398. 2022. doi: 10.1063/5.0094037. University of Kirkuk.
15. A. Ghaleb, B. Yamina, A. Ahmed, and Z. Talib, "STRUCTURAL, ELECTRONIC, AND OPTICAL PROPERTIES INVESTIGATION OF ZnSe CUBIC SPHALERITE COMPOUNDS USING DENSITY FUNCTIONAL THEORY (DFT)," Probl. At. Sci. Technol., pp. 103–109, Jan. 2024, doi: 10.46813/2024-149-103. University of Kirkuk.

International Journal of Applied and Structural Mechanics
ISSN: 2799-127X
Vol: 04, No. 05, August-September 2024
http://journal.hmjournals.com/index.php/IJASM
DOI: https://doi.org/10.55529/ijasm.45.11.24

16. A. M. Ghaleb and A. Q. Ahmed, "Structural, electronic, and optical properties of sphalerite ZnS compounds calculated using density functional theory (DFT)," vol. 19, no. 5, pp. 309–318, 2022. University of Kirkuk.
17. Z. Usman, C. Cao, G. Nabi, D. Y. Kun, W. S. Khan, and T. Mehmood, "First-Principle Electronic, Elastic, and Optical Study of Cubic Gallium Nitride," pp. 6622–6628, 2011.
18. M. B. Kanoun, S. Goumri-Said, A. E. Merad, G. Merad, J. Cibert, and H. Aourag, "Zinc-blende AlN and GaN under pressure: structural, electronic, elastic and piezoelectric properties," Semicond. Sci. Technol., vol. 19, no. 11, p. 1220, 2004.
19. S. Li and C. Ouyang, "First principles study of wurtzite and zinc blende GaN: a comparison of the electronic and optical properties," Phys. Lett. A, vol. 336, no. 2–3, pp. 145–151, 2005.
20. A. M. Ghaleb, Y. Benkrima, A. Q. Ahmed, and Z. T. Ghaleb, "STRUCTURAL , ELECTRONIC , AND OPTICAL PROPERTIES INVESTIGATION OF ZnSe CUBIC SPHALERITE COMPOUNDS USING DENSITY FUNCTIONAL THEORY (DFT)," vol. 1, no. 149, pp. 103–109, 2024.
21. M. D. Segall et al., "First-principles simulation: ideas, illustrations and the CASTEP code," J. Phys. Condens. Matter, vol. 14, no. 11, p. 2717, 2002.
22. D. Vanderbilt, "Soft self-consistent pseudopotentials in a generalized eigenvalue formalism," Phys. Rev. B, vol. 41, no. 11, p. 7892, 1990.
23. S. H. Vosko, L. Wilk, and M. Nusair, "Accurate spin-dependent electron liquid correlation energies for local spin density calculations: a critical analysis," Can. J. Phys., vol. 58, no. 8, pp. 1200–1211, 1980.
24. J. P. Perdew, J. Tao, V. N. Staroverov, and G. E. Scuseria, "Meta-generalized gradient approximation: Explanation of a realistic nonempirical density functional," J. Chem. Phys., vol. 120, no. 15, pp. 6898–6911, 2004.
25. D. Sanchez-Portal, E. Artacho, and J. M. Soler, "Projection of plane-wave calculations into atomic orbitals," Solid State Commun., vol. 95, no. 10, pp. 685–690, 1995.
26. M. D. Segall, R. Shah, C. J. Pickard, and M. C. Payne, "Population analysis of plane-wave electronic structure calculations of bulk materials," Phys. Rev. B, vol. 54, no. 23, p. 16317, 1996.
27. T. Lei, T. D. Moustakas, R. J. Graham, Y. He, and S. J. Berkowitz, "Epitaxial growth and characterization of zinc-blende gallium nitride on (001) silicon," J. Appl. Phys., vol. 71, no. 10, pp. 4933–4943, 1992.
28. C. Stampfl and C. G. Van De Walle, "Density-functional calculations for III-V nitrides using the local-density approximation and the generalized gradient approximation," vol. 59, no. 8, 1999.
29. W. H. Moon and H. J. Hwang, "Structural and thermodynamic properties of GaN: a molecular dynamics simulation," Phys. Lett. A, vol. 315, no. 3–4, pp. 319–324, 2003.
30. M. Leszczynski et al., "Lattice parameters of gallium nitride," Appl. Phys. Lett., vol. 69, no. 1, pp. 73–75, 1996.
31. A. F. Wright and J. S. Nelson, "Explicit treatment of the gallium 3d electrons in GaN using the plane-wave pseudopotential method," Phys. Rev. B, vol. 50, no. 4, p. 2159, 1994.

International Journal of Applied and Structural Mechanics
ISSN: 2799-127X
Vol: 04, No. 05, August-September 2024
http://journal.hmjournals.com/index.php/IJASM
DOI: https://doi.org/10.55529/ijasm.45.11.24

32. M. Magnuson, M. Mattesini, C. Höglund, J. Birch, and L. Hultman, "Electronic structure of GaN and Ga investigated by soft x-ray spectroscopy and first-principles methods," Phys. Rev. B, vol. 81, no. 8, p. 85125, 2010.
33. A. Janotti, D. Segev, and C. G. Van de Walle, "Effects of cation d states on the structural and electronic properties of III-nitride and II-oxide wide-band-gap semiconductors," Phys. Rev. B, vol. 74, no. 4, p. 45202, 2006.
34. A. Rubio, J. L. Corkill, M. L. Cohen, E. L. Shirley, and S. G. Louie, "Quasiparticle band structure of AlN and GaN," Phys. Rev. B, vol. 48, no. 16, p. 11810, 1993.
35. S. Q. Wang and H. Q. Ye, "A plane-wave pseudopotential study on III–V zinc-blende and wurtzite semiconductors under pressure," J. Phys. Condens. Matter, vol. 14, no. 41, p. 9579, 2002.
36. B. Luo, X. Wu, and G. Li, "Electronic structure, elastic and thermal properties of semiconductor GaX (X= N, P, As, Sb) with zinc blende from first-principles calculation," Int. J. Mod. Phys. B, vol. 28, no. 27, p. 1450183, 2014.
37. T. Kawashima, H. Yoshikawa, S. Adachi, S. Fuke, and K. Ohtsuka, "Optical properties of hexagonal GaN," J. Appl. Phys., vol. 82, no. 7, pp. 3528–3535, 1997.
38. Y. Zhang and J. Zhang, "First principles study of structural and thermodynamic properties of zirconia," Mater. Today Proc., vol. 1, no. 1, pp. 44–54, 2014.
39. E. Tuncel, K. Colakoglu, E. Deligoz, and Y. O. Ciftci, "A first-principles study on the structural, elastic, vibrational, and thermodynamical properties of BaX (X= S, Se, and Te)," J. Phys. Chem. Solids, vol. 70, no. 2, pp. 371–378, 2009.
40. O. L. Anderson, "A simplified method for calculating the Debye temperature from elastic constants," J. Phys. Chem. Solids, vol. 24, no. 7, pp. 909–917, 1963.
41. P. Ravindran, L. Fast, P. A. Korzhavyi, B. Johansson, J. Wills, and O. Eriksson, "Density functional theory for calculation of elastic properties of orthorhombic crystals: Application to TiSi 2," J. Appl. Phys., vol. 84, no. 9, pp. 4891–4904, 1998.
42. J. Petalas, S. Logothetidis, S. Boultadakis, M. Alouani, and J. M. Wills, "Optical and electronic-structure study of cubic and hexagonal GaN thin films," Phys. Rev. B, vol. 52, no. 11, p. 8082, 1995.